Using patterned H-resist for controlled three-dimensional growth of nanostructures

K. E. J. Goh,[1,a)] S. Chen,[2] H. Xu,[2,b)] J. Ballard,[3] J. N. Randall,[3] and J. R. Von Ehr[3]
[1]*Institute of Materials Research and Engineering, Agency for Science, Technology and Research (A*STAR), 3 Research Link, Singapore 117602*
[2]*Zyvex Asia Pte Ltd, 3 Research Link, Singapore 117602*
[3]*Zyvex Labs LLC, Richardson, Texas 75081, USA*

(Received 10 February 2011; accepted 4 April 2011; published online 18 April 2011)

We present a study addressing the effectiveness of a monolayer of hydrogen as the lithographic resist for controlled three-dimensional (3D) growth of nanostructures on the Si(100) surface. Nanoscale regions on the H-terminated Si(100) were defined by H-desorption lithography via the biased tip of a scanning tunneling microscope (STM) to create well-defined regions of surface "dangling bonds," and the growth of 3D nanostructures within these regions was achieved using a simultaneous disilane deposition and STM H-desorption technique. We demonstrate that 3D growth is strongly confined within STM depassivated regions while unpatterned H:Si(100) regions are robust against adsorption of the precursor molecules. © *2011 American Institute of Physics*. [doi:10.1063/1.3582241]

The patterning of H-terminated Si(100) by the scanning tunneling microscope (STM) was first reported by Lyding *et al.*[1] in 1994. Since then, this technique of using H as a lithographic resist has been studied in conjunction with the use of various precursor molecules to achieve selective adsorption of the molecules on Si(100).[2,3] In particular, there has been considerable interest in recent times to use this technique to achieve atomic precision planar doping in Si(100) with the objective of fabricating low-dimensional devices including nanowires, tunnel-junctions, few-electron quantum dots, and ultimately single dopant devices which form the qubits of a quantum computer.[4–6] While these works demonstrate that the H-resist is effective for achieving atom-level control for the fabrication of planar nanostructures, it remains unclear if the patterned H-resist could also be effectively used for the controlled growth of nanostructures in all three dimensions. Here, we present a study investigating the use of the H-resist to achieve controlled three-dimensional (3D) growth of nanostructures on Si(100). We found that the H-resist provided a high degree of selectivity for controlled 3D growth at room temperature when used in conjunction with disilane molecules as growth precursors, highlighting the potential of this technique for achieving atomically precise structures in 3D.

The experiment was performed in a home-built ultrahigh vacuum STM system (base pressure of 2×10^{-10} torr), complete with gas lines for high purity (99.999%) H and disilane (Si_2H_6) gas sources. The substrates were P-doped n-Si(100) wafers (resistivity ~0.01 Ω cm, <0.1° miscut, ~2 mm wide, and ~10 mm long) cleaned in the preparation chamber by overnight degassing at ~600 °C followed by three cycles of flash anneal to ~1150 °C for about 30 s while maintaining a chamber pressure of $<1\times10^{-9}$ torr. H-termination was performed by back-filling the preparation chamber with H_2 to a pressure of $\sim5\times10^{-7}$ torr and cracking the H_2 over a hot tungsten filament near but not in direct line-of-sight to the sample which was held at ~365 °C. This procedure resulted in H:Si(100) surface having typically monohydride coverages of >95% with the remaining few percent comprising mainly single "dangling bonds" which do not facilitate the dissociative chemisorption of Si_2H_6, a process requiring a least 2 contiguous dangling bonds on Si(100) at room temperature.[7–9] The H:Si(100) sample was subsequently transferred into the STM chamber for imaging, lithography and growth studies. All STM imaging and H-lithography were performed with a W-tip prepared by annealing to ~830 °C for 30 min to remove the oxide layer.

Figure 1 shows representative height profiles (along line-scans indicated by arrows) and the corresponding STM images for the starting H:Si(100), STM patterned 100×100 nm^2 (nominal) depassivated Si(100) region, and various stages of growth within the same region. The height profile for the H:Si(100) starting surface shows a step of (1.34 ± 0.06) Å, in good agreement with a single terrace step on the Si(100) surface.[8] During STM lithography, H-desorption was performed under feedback control using a tip bias of −7 V and a tunneling current of 0.5 nA, with a line-scan speed achieving an estimated dose of 0.5 mC cm^{-1}. These conditions resulted in effectively continuous depassivation over the 100×100 nm^2 region as shown in Fig. 1, with the dangling bonds showing typical protrusions of (1.3 ± 0.2) Å above the H:Si(100) surface.[3,10]

For Si growth, disilane was leaked into the STM chamber via a precision leak valve to achieve a dosing pressure of 1×10^{-8} torr at room temperature, and the STM tip was continuously rastered across the 100×100 nm^2 region with the same conditions as for H-desorption. Upon exposure to Si_2H_6, the highly reactive dangling bonds exposed by STM lithography can capture Si_2H_6 molecules which progressively dissociate into SiH_3 fragments and subsequently SiH_2 and H,[7,8] forming a self-terminating growth front due to the presence of passivating H—this is the generally accepted picture of the dissociative chemisorption of Si_2H_6 on Si(100), however the exact mechanism remains an area of controversy and on-going research.[7–9,11] Simultaneous rastering of the STM tip using H-desorption conditions therefore served to remove H from the growth front, allowing further

a)Electronic mail: kejgoh@yahoo.com.
b)Electronic mail: hxu@zyvexasia.com.

 © 2011 American Institute of Physics

Author complimentary copy. Redistribution subject to AIP license or copyright, see http://apl.aip.org/apl/copyright.jsp

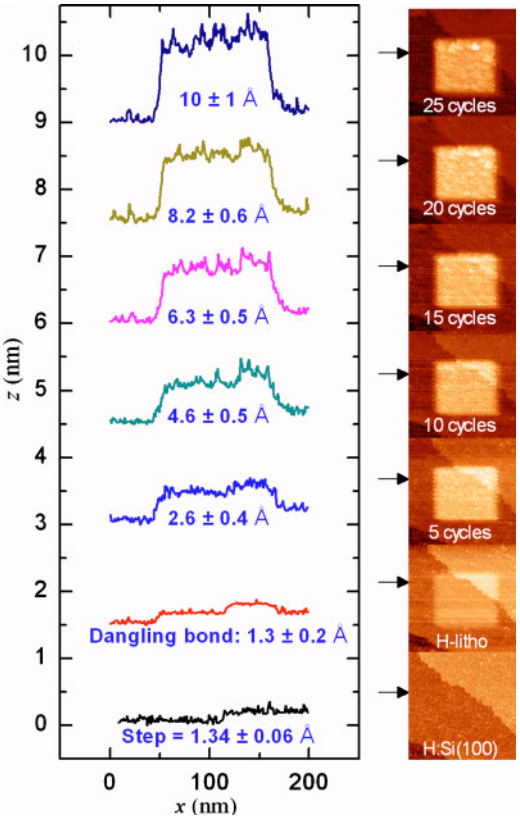

FIG. 1. (Color online) STM images (200×200 nm^2) showing the starting H:Si(100) surface, patterning by STM H-depassivation to form the nominally 100×100 nm^2 square, and the same patterned region after 5, 10, 15, 20, and 25 lithography-deposition cycles. Imaging conditions were −2.2 V and 0.1 nA. The line profiles (offset vertically) on the left are taken along line-scans over the same line in each image indicated by the arrow.

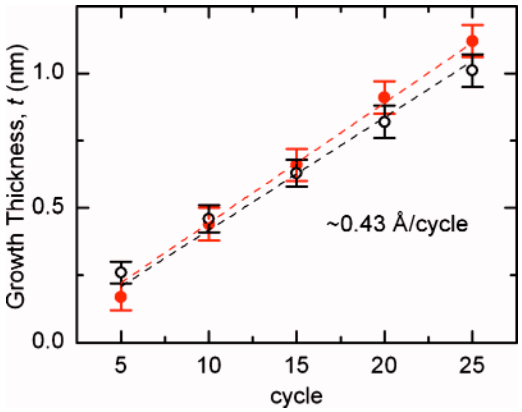

FIG. 2. (Color online) Graphs of deposition thickness (t) against the number of lithography-deposition cycles for the 100×100 nm^2 (black, open circles) and the 20×20 nm^2 (red, solid circles) patterned regions.

layers of Si to grow. Each complete raster over the 100×100 nm^2 region took 120 s and constitutes a growth cycle. Growth was interrupted (by closing the disilane leak valve) immediately after 5, 10, 15, 20, and 25 cycles for STM imaging. Previous studies on Si homoepitaxy have shown that low temperature Si epitaxy is thickness limited for a given growth rate and epitaxy is possible for up to a few nm at room temperature using a growth rate of 0.7 Å s^{-1} and the epitaxial thickness is expected to be greater at lower growth rates.[12,13] However, these studies were based on molecular beam epitaxy where the adatoms are likely more energetic and Si growth is not limited by the same chemisorption mechanics as for gas phase growth by Si_2H_6. The "epitaxial thickness" for Si growth using Si_2H_6 is therefore expected to be significantly reduced. In the present case, we have stopped the growth after achieving a thickness of about 1 nm for the room temperature gas phase deposition using a relatively low rate of ~0.0036 Å s^{-1} (see Fig. 2 and discussions below). However, the W-tip used in this work was not capable of atomic resolution after the growth cycles (likely due to the presence of adsorbates on the W-tip), making it difficult to ascertain the actual growth quality via STM imaging. The general growth profile over the 100×100 nm^2 region was less impacted by the tip sharpness and is therefore used provide an assessment of the effectiveness of the lithographically confined growth process.

The representative growth profiles in Fig. 1 show a progressively rougher growth front as the number of growth cycles increases. This is likely due to a combination of the random landing of the fragments from Si_2H_6 and the exclusion of Si_2H_6 landing in regions lacking the minimum number of required dangling bonds. It is also possible that H fragments left from the dissociation of Si_2H_6 could impede adatom diffusion and hence impact nucleation and island growth. However, this latter effect should be significantly minimized by the STM H-desorption in each growth cycle. At room temperature, the growth front is most likely amorphous although some rearrangements of the Si adatoms might occur after H-desorption in each cycle. In Fig. 1, the line-scans were performed in the horizontal direction with respect to the images. Although H-desorption in the growth region was performed line-by-line, the STM images indicate that the growth thickness over the entire region of interest was essentially constant at each inspection cycle. This implies that during each cycle of simultaneous H-desorption and Si_2H_6 deposition, the Si deposited remained sufficiently passivated[14] to form a self-terminating growth front, and effectively no further growth occurred until the STM tip came along in the next cycle to remove H and allow the next layer of Si to be deposited. The STM images in Fig. 1 further show that the H-resist surrounding the STM-patterned region remained impervious throughout the 25 growth cycles. Overall, the above results indicate that the H-resist provided excellent selectivity for laterally confined Si growth, and the line-by-line simultaneous H-desorption and Si_2H_6 deposition technique employed here provided relatively uniform areal growth cycles. It is probably worth mentioning that some growth artifacts begin to appear in the top-right quadrant of the growth region for images of the 20th cycle and beyond. This is likely due to fragments (possibly amorphous clusters containing Si and H) deposited by the tip directly onto the growth region some time between the 15th and 20th cycle. In assessing the growth thickness, we have taken care to avoid these artifacts.

In Fig. 2, we plot the average growth thickness as a function of the number of lithography-deposition cycles (black open circles). The growth thickness appears to vary linearly up to the maximum of 25 cycles in this study, with a rate of ~0.43 Å/cycle (or ~0.0036 Å s^{-1}). Based on this growth rate, one would expected to grow a full monolayer of Si (assuming a full monolayer coverage here has a surface atom density roughly similar to a ~1.36 Å thick[8] Si(100) surface monolayer) in about three cycles. Reports by Wang *et al.*[8] and Que *et al.*[9] indicate that at low surface coverages,

Author complimentary copy. Redistribution subject to AIP license or copyright, see http://apl.aip.org/apl/copyright.jsp

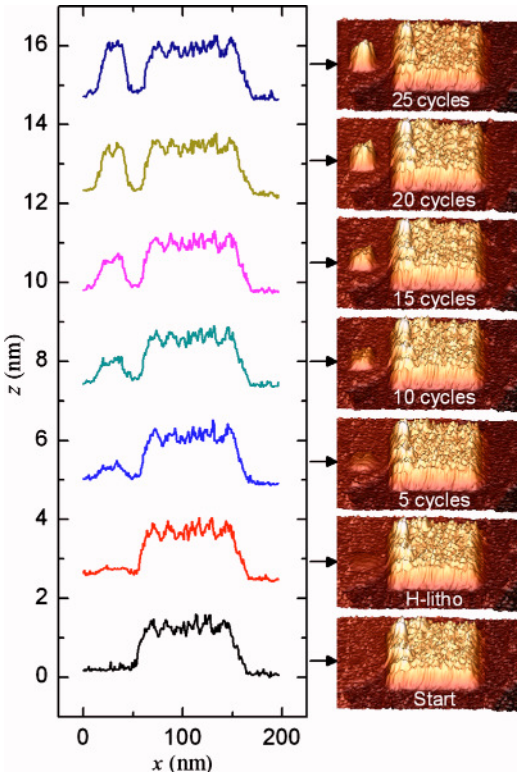

FIG. 3. (Color online) Representative height profiles (offset vertically) and 3D orthogonal relief representation of the pregrown $1\times100\times100$ nm^3 nanostructure, and second nanostructure growing in the 20×20 nm^2 patterned region. Imaging conditions were −2.2 V and 0.1 nA. Arrows indicate line profile positions taken in a direction orthogonal to that of the line profiles in Fig. 1. Here, the different slopes of the side walls are attributable to asymmetry in the tip shape.

SiH_3 fragments have sufficient dangling bond sites to further dissociate into SiH_2 and H resulting in two Si adatoms for every six dangling bonds consumed, while at high coverages SiH_3 fragments could not dissociate further due to stronger competition for dangling bonds resulting in two Si adatoms for every two to four dangling bonds consumed (depending on how the SiH_3 bond to a dimer). The ~0.33 monolayer per cycle achieved with our growth conditions appear to provide support for the low coverage scenario.

To further test the robustness of the H-resist and the reproducibility of the Si growth, we attempted a similar growth over a smaller nominally 20×20 nm^2 region adjacent to the first one. The actual position of the smaller structure is just above the larger structure grown in Fig. 1. Inspection of the growth by STM imaging was again performed immediately after 5, 10, 15, 20, and 25 growth cycles. To obtain a better viewing angle for assessing the growth progression of the smaller structure and the integrity of the pregrown larger structure, we have rotated the scan frame counter-clockwise by 90° in Fig. 3. Here, together with the 3D orthogonal relief representation of both structures, we also provide a representative line profile (along the directions indicated by the arrows) tracking the growth of the smaller structure as well as the any change in the larger structure over 25 growth cycles. Figure 3 clearly shows that the larger structure remained unaltered in all three dimensions throughout the extra 25 growth cycles. In addition, there is again no evidence that the surrounding H-resist was compromised. The average growth thickness against the number of growth cycles for this smaller structure is plotted (red solid circles) in Fig. 2 and shows essentially the same behavior/rate as that for the larger structure. Interesting, the tip again appears to "drop" a cluster onto the growth region from around the 20th cycle. These preliminary observations suggest that a possible critical mass of material accumulated on the tip over the course of about 20 growth cycles, became unstable, and detached from the tip. However, this postulate requires further experiments to establish and is beyond the scope of this letter. Nonetheless, we have shown that the same combination of lithography and growth conditions can also work well for the smaller region, and the fact that the larger structure remained intact indicates that such nanostructures need not be grown at the same time. This opens the possibility for creating more complex 3D nanostructure arrays such as those comprising structures with varying heights, or multilevel pyramidal structures with differing structures at each level.

In conclusion, the above experiments demonstrate that the monolayer H-resist can indeed be an effective mask against Si_2H_6 adsorption at room temperature, and together with STM H-desorption lithography and Si_2H_6 as the growth precursor, can be used to effectively control Si growth in all three dimensions to achieve well-defined nanostructures down to few tens of nm in size. While this work marks significant progress toward creating atomically precise 3D nanostructures using the said technique, it also highlights the importance of further development to achieve robust STM tips and a good understanding of how the tip is modified while under use.

This work was supported by funding from Zyvex Laboratories LLC (USA), A*STAR (Singapore) under the Project No. IMRE/08-1P0102, and the Defense Advanced Research Project Agency (DARPA) Contract No. N66001-08-C-2040.

[1]J. W. Lyding, T.-C. Shen, J. S. Hubacek, J. R. Tucker, and G. C. Abeln, Appl. Phys. Lett. **64**, 2010 (1994).
[2]M. C. Hersam, N. P. Guisinger, and J. W. Lyding, Nanotechnology **11**, 70 (2000).
[3]K. E. J. Goh, L. Oberbeck, M. J. Butcher, N. J. Curson, F. J. Rueß, and M. Y. Simmons, Nanotechnology **18**, 065301 (2007).
[4]F. J. Rueß, W. Pok, T. C. G. Reusch, M. J. Butcher, K. E. J. Goh, G. Scappucci, A. R. Hamilton, and M. Y. Simmons, Small **3**, 563 (2007); F. J. Rueß, K. E. J. Goh, M. J. Butcher, T. C. G. Reusch, L. Oberbeck, B. Weber, A. R. Hamilton, and M. Y. Simmons, Nanotechnology **18**, 044023 (2007).
[5]M. Y. Simmons, F. J. Rueß, K. E. J. Goh, W. Pok, T. Hallam, M. J. Butcher, T. C. G. Reusch, and G. Scappucci, Int. J. Nanotechnol. **5**, 352 (2008).
[6]M. Fuechsle, S. Mahapatra, F. A. Zwanenburg, M. Friesen, M. A. Eriksson, and M. Y. Simmons, Nat. Nanotechnol. **5**, 502 (2010).
[7]M. J. Bronikowski, Y. Wang, M. T. McEllistrem, D. Chen, and R. J. Hamers, Surf. Sci. **298**, 50 (1993).
[8]Y. Wang, M. J. Bronikowski, and R. J. Hamers, Surf. Sci. **311**, 64 (1994).
[9]J.-Z. Que, M. W. Radny, and P. V. Smith, Phys. Rev. B **60**, 8686 (1999).
[10]Y. Wang, M. J. Bronikowski, and R. J. Hamers, J. Vac. Sci. Technol. A **12**, 2051 (1994).
[11]R. Q.-M. Ng, E. S. Tok, and H. C. Kang, J. Chem. Phys. **130**, 114702 (2009).
[12]D. J. Eaglesham, J. Appl. Phys. **77**, 3597 (1995).
[13]K. E. J. Goh, L. Oberbeck, M. Y. Simmons, A. R. Hamilton, and R. G. Clark, Appl. Phys. Lett. **85**, 4953 (2004).
[14]After the dissociative chemisorption of Si_2H_6 on the lithographically depassivated Si surface, the growth front will predominantly comprise dihydride or monohydride passivated Si adatoms depending on whether the chemisorbed SiH_2 fragments dissociate further. Single "dangling bonds" are also likely left unpassivated at this growth front due to limited H-mobility and the improbability for Si_2H_6 adsorption at such sites at room temperature.

Author complimentary copy. Redistribution subject to AIP license or copyright, see http://apl.aip.org/apl/copyright.jsp